Supplementary File

Structure of tRNA methyltransferase complex of Trm7 and Trm734 reveals a novel binding interface for tRNA recognition

Akira Hirata[1*], Keisuke Okada[1*], Kazuaki Yoshii[1], Hiroyuki Shiraishi[1], Shinya Saijo[2], Kento Yonezawa[2], Nobutaka Shimizu[2], and Hiroyuki Hori[1]

*These authors equally contributed to this work.

[1] Department of Materials Science and Biotechnology, Graduate school of Science and Engineering, Ehime University, 3 Bunkyo-cho, Matsuyama, Ehime 790-8577, Japan

[2] Photon Factory, Institute of Materials Structure Science, High Energy Accelerator Research Organization (KEK) 1-1 Oho, Tsukuba, Ibaraki 305-0801, Japan

To whom correspondence should be addressed:
Hiroyuki Hori,
Department of Materials Science and Biotechnology, Graduate School of Science and Engineering, Ehime University, 3 Bunkyo-cho, Matsuyama, Ehime 790-8577, Japan.
Phone: 81-89-927-8548
e-mail: hori.hiroyuki.my@ehime-u.ac.jp

SUPPORTING MATERIALS AND METHODS

Construction of expression vectors

The *trm7* gene was amplified by polymerase chain reaction (PCR) with two primers (trm7F and trm7R), and then ligated into a TA-cloning vector pMD20-T by using a Mighty TA-cloning kit (TAKARA, Japan). For the construction of expression system of Trm7 in *E. coli* BL21 (DE3) Rosetta 2 strain, the *trm7* gene was further inserted between T7 promotor and terminator in the expression vector pET30a (Novagen) using the In-Fusion HD Cloning Kit (Clontech) with the four primers (in-trm7F, in-trm7R, pE30F and pE30R). The primer of in-trm7R includes sequences of 6×His-tag with HRV-3C protease site at the C-terminal of Trm7. For the construction of co-expression systems of Trm7-Trm732 and Trm7-Trm734 in *E. coli* BL21 (DE3) Rosetta 2 strain, the *trm7* gene was initially inserted between T7 promotor and terminator in the expression vector pET21a (Novagen) using the primers (in-trm7F, in-trm7R, pE21F and pE21R). The *trm732* and *trm734* genes are amplified by PCR, and then inserted between T7 promotor and terminator in the pET21a, respectively, with the following primers, in-trm732F, in-trm732R, in-trm734F, in-trm734R, pE21F and pE21R. The primers of in-trm732R and in-trm734R include sequences of 6×His-tag at the C-terminal of Trm732 and Trm734. The

amplified *trm732* and *trm734* genes by PCR, which include the T7 promotor at the upstream of each gene in the pET21a, were, respectively, inserted into the site between the stop codon of *trm7* gene and T7 terminator in the pET21a harboring *trm7* gene by using the in-fusion system with the primers (trm7-vecF, trm7-vecR, coex-inF, coex-inR32 and coex-inR34). The constructions of co-expression plasmids harboring *trm7-trm732* or *trm7-trm734* genes were verified by DNA sequencing.

Small angle X-ray scattering (SAXS) data collection and processing

Prior to the measurement of SAXS data, the concentrated samples were loaded onto a Superdex 200 column (GE Healthcare) equilibrated with the buffer [50 mM HEPES-KOH (pH 8.0), 10 mM 2-mercaptoethanol, 200mM KCl and 5% Glycerol], and the eluted samples were diluted with the buffer to each final concentration as shown in Table S4A. The concentration variation series of apo Trm7-Trm734 were loaded into a stainless-steel cell of 1.25 mm light pass with a 0.02 mm-thick quartz glass window. These samples were measured at 6 different concentrations (details are shown in Table S4A) in the same buffer. Ovalbumin (45 kDa; Sigma-Aldrich) was also measured for estimation of the apparent molecular weight. The scattering intensities (I(Q)) were measured in the region of approximately $0.01 < Q < 0.4$ Å^{-1},

where $Q = 4\pi \sin\theta/\lambda$ and $\lambda = 1$ Å, at the distance between sample and detector of about 2 m (Table S4B). The exposure times and the number of images were 10 sec and 40 images. The scattering images were recorded on a PILATUS3 2M detector (Dectris). Each scattering image was circularly averaged and converted to the scattering intensity profiles and subtracted background by *SAngler* software (1). Sample radiation damages were monitored by data frame-by-frame comparison. The scattering intensities converted to an absolute scale were used by water scattering as a standard. Extrapolation to zero concentration was performed by the program *PRIMUSqt* of the program package *ATSAS* (2-4). Scattering intensities at zero angle ($I(0)$) and radius of gyration (R_g) were calculated under the condition of Guinier approximation by using *AUTORG* (5). The pair distribution function ($P(r)$) was obtained by using *GNOM* and maximum size parameter (D_{max}) was estimated based on $P(r)$ function (6). Molecular Weights from $I(0)$ are calculated by using *SAXSMoW* (v2.1) (7). Profiles attribute to scattering experiment are shown in Supplementary Figure S5 and Table S4D.

Automatic *ab initio* modeling was performed by using the DAMMIF module of *PRIMUSqt*. In this module, the program *DAMMIF* (8) firstly generated 20 dummy atom models and the program *DAMAVER* (9) secondary averaged these models. Finally, the program *DAMMIN*

(10) generated the final model with the initial model that *DAMAVER* outputted. In order to optimize the position of Trm7 including terminal linkers (residue 1-8 and 260-310) and Trm734 by rigid body modeling, crystal structures of these domains separated from crystal structures (PDB) were used to fit SAXS scattering data using program *CORAL* (2). According to our obtained X-ray crystal structure, approximate positions were limited by contacts (contact positions are described in Table S4F). The obtained rigid body models were superimposed on the dummy atom model using the program *SUPCOMB* (11). The structure obtained from *CORAL* (Figure 1C) was drawn by *Chimera* ver 1.12 (12). This structure information is submitted to small angle scattering biological data bank (SASBDB; https://www.sasbdb.org/aboutSASBDB/) (13). Deposited SASBDB ID is SASDDR3.

In addition to SAXS data of apo Trm7-Trm734, that of Trm7-Trm734 in complex with $tRNA^{Phe}$ and sinefungin was also obtained on the BL45XU beamlines at SPring-8 (Hyogo, Japan). The method for the sample preparation of this complex was the same with that of apo Trm7-Trm734. Five concentration variation series of the Trm7-Trm734-$tRNA^{Phe}$ complex was load into a cuvette of 3 mm light pass with a 0.02 mm-thick quartz glass window (shown in Table S4A). The scattering intensities of the Trm7-Trm734-$tRNA^{Phe}$ complex in almost the

same region of Trm7-Trm734 were recorded on a PILATUS 300K-W detector (Dectris), where the wavelength and the camera distance are 1 Å and about 2 m respectively (Table S4B). The exposure times and the number of images were set to 1 sec and 20 images respectively. The procedure and the software for data processing and analyses are the same as those of apo Trm7-Trm734. Resultant profiles and Guinier analyses are also shown in Supplementary Figure S5 and Table S4D.

REFERENCES in Supplementary file

1. Shimizu, N., Nagatani, Y., S. Kosuge, T. and Igarashi, N. (2016) Software development for analysis of small-angle x-ray scattering data. *AIP Conference Proceedings,* **1741,** 050017.
2. Franke, D., Petoukhov, M. V., Konarev, P. V., Panjkovich, A., Tuukkanen, A., Mertens, H. D. T., Kikhney, A. G., Hajizadeh, N. R., Franklin, J. M., Jeffries, C. M. *et al.* (2017) ATSAS 2.8: a comprehensive data analysis suite for small-angle scattering from macromolecular solutions. *J. Appl. Crystallogr*., **50**, 1212-1225.
3. Petoukhov, M. V., Franke, D., Shkumatov, A. V., Tria, G., Kikhney, A. G., Gajda, M., Gorba, C., Mertens, H. D., Konarev, P. V. and Svergun, D. I. (2012) New developments in the ATSAS program package for small-angle scattering data analysis. *J. Appl. Crystallogr.*, **45**, 342-350.
4. Konarev, P. N., Volkov, V. V., Sokolova, A. V., Kock, M. H. and Svergun, D. I. (2003) *PRIMUS*: a Windows PC-based system for small-angle scattering data analysis. *J. Appl. Crystallogr.*, **36**, 1277-1282.
5. Petoukhov, M. V., Konarev, P. V., Kikhney, A. G. and Svergun, D. I. (2007) ATSAS 2.1 - Towards automated and web-supported small-anglescattering data analysis. *J. Appl. Crsytallogr.*, **45**, 223-228.
6. Svergun, D. I. (1992) Determination of the regularization parameter inindirect-transform methods using perceptual criteria. *J. Appl. Crystallogr.*, **25**, 495-503.
7. Fischer, H., De Oliveira Neto, M., Napolitano, H. B., Polikarpov, I. and Graievich, A. F. (2010) Determination of the molecular weight of proteins in solutionfrom a single small-angle X-ray scattering measurement on a relative scale. *J. Appl. Crystallogr.*, **43**, 101-109.
8. Franke, D. and Svergun, D. I. (2009) DAMMIF, a program for rapid ab-initio shape determination insmall-angle scattering. *J. Appl. Crystallogr.*, **36**, 860-864.
9. Volkov, V. V. and Svergun, D. I. (2003) Uniqueness of ab initio shape determination in small-anglescattering. *J. Appl. Crystallogr.*, **36**, 860-864.
10. Svergun, D. I. (1999) Restoring low resolution structure of biological macromolecules from solution scattering using simulated annealing. *Biophys J.*, **76**, 2879-2886.
11. Kozin, M. B. and Svergun, D. I. (2001) Automated matching of high- and low-resolution structuralmodels. *J. Appl. Crystallogr.*, **34**, 33-41.
12. Pettersen, E. F., Goddard, T. D., Huang, C. C., Couch, G. S., Greenblatt, D. M., Meng, E. C.

and Ferrin, T. E. (2004) UCSF Chimera--a visualization system for exploratory research and analysis. *J. Comput. Chem.*, **25**, 1605-1612.

13. Svergun, D., Barbetato, C. and Koch, M. H. (1995) CRYSOL - A program to evaluate X-ray solution scattering ofbiological macromolecules from atomic coordinates. *J. Appl. Crystallogr.*, **28**, 768-773.
14. Valentini, E., Kikhney, A. G., Previtali, G., Jeffries, C. M. and Svergun, D. I. (2015) SASBDB, a repository for biological small-angle scattering data. *Nucleic Acids Res.*, **43**, D357-363.
15. Chenna, R. *et al.* Multiple sequence alignment with the Clustal series of programs. (2003) *Nucleic Acids Res.*, **31**, 3497-3500.
16. Gouet, P., Robert, X.and Courcelle, E. ESPript/ENDscript: Extracting and rendering sequence and 3D information from atomic structures of proteins. (2003) *Nucleic Acids Res.*, **31**, 3320-3323.

Supplementary Table S1.

Primers for the constructions of co-expression vectors for Trm7-Trm732 and Trm7-Trm734

trm7F

Forward

5′-ATGGGTAAGAGCAGCAAAGATAAAAGAGAT-3′

trm7R

Reverse

5′-TCAAACTGATCTAGTGAGTTTCCCGC-3′

in-trm7F

Forward

5′-AGAAGGAGATATACATATGGGTAAAGAGCAGCAAAGATAAAAGAGA TTG-3′

in-trm7R

Reverse

5′-ATGGTGATGGTGATGGGAGGGTCCCTGAAAGAGGACTTCAAGAACT

GATCTAGTGAGTTTCCCGCTCCTTTTTAA-3′

in-trm732F

Forward

5′-AGAAGGAGATATACATATGACTACGGATGTGCAATTTTCAAGTCAGGA AAT-3′

in-trm732R

Reverse

5′-ATGGTGATGGTGATGTAATTGGGAATAACTGATAATTAGGGGATGAAC AGAAT-3′

in-trm734F

Forward

5′-AGAAGGAGATATACATATGAAGGACTTGTCTCATTATGGTCCTGC-3′

in-trm734R

Reverse

5′-ATGGTGATGGTGATGTTTTTTCCAAATTGATAAACCAACACCTCCGAT CAG-3′

trm7-VecF

Forward

5′-GGATCCGAATTCGAGCTCCGTCG-3′

trm7-VecR

Reverse

5′-TTAGTGATGGTGATGGTGATGGGAGG-3′

coex-inF

Forward

5′-CATCACCATCACTAATAATACGACTCACTATAGGGGAATTGTGAGC-3′

coex-inR32

Reverse

5′-CTCGAATTCGGATCCTTAGTGATGGTGATGGTGATGTAATTGGGAATA A-3′

coex-inR34

Reverse

5′-CTCGAATTCGGATCCTTAGTGATGGTGATGGTGATGGTGATGTTTTT

TCCAAATTG-3′

pE30F

Forward

5′-TGAGGATCCGAATTCGAGCTCCGT-3′

pE30R

Reverse

5′-CATATGTATATCTCCTTCTTAAAGTTAAACAAAATTATTTC-3′

pE21F

Forward

5′-CATCACCATCACCATCACTAAGGATCCG-3′

pE21R

Reverse

5′-ATGTATATCTCCTTCTTAAAGTTAAACAAAATTATTTCTAGAGGG-3′

The bold show a primers name. homologous recombination sequences colored red. The green sequences denote a HRV3C-protease site in the primer of in-trm7R. The homologous recombination sequences of in-trm732R and in-trm734R primers are comprised of 6×His-tag sequences.

Supplementary Table S2.

Primers list for the constructions of A26P mutant and deletion mutants ($\Delta_{233\text{-}310}$ Trm7 and $\Delta_{260\text{-}310}$ Trm7).

A26P

Forward

5′-CTATAGGGCTAGATCTCCGTTCAAACTACTTCAAC-3′

Reverse

5′-GTTGAAGTAGTTTGAACGGAGATCTAGCCCTATAG-3′

Deletion ($\Delta_{233\text{-}310}$ Trm7)

Forward

CAAAAAACAGCCTTGAAAAAATTCATC

Reverse

CTTGAAGTCCTCTTTCAGGGACC

Deletion ($\Delta_{260\text{-}310}$ Trm7)

Forward

5′-AGTCTTCAAAGTTTCGACTCAGATGCCACTTATC-3′

Reverse

5′-TCCACAAGCCATAAATTCGGCTATGTTTCTCTCC-3′

The bold show a primers name. Mutational sequences colored red.

Supplementary Table S3.

Primers for the transcriptions of *S. cerevisiae* $tRNA^{Phe}$ transcript, $tRNA^{Trp}$ transcript and $tRNA^{Phe}$ mutants

$tRNA^{Phe}$ transcript

Forward

5′-**GGGTAATACGACTCACTATA**GCGGATTTAGCTCAGTTGGGAGAGCGC CAGACTGAAGATCTGGAGGTC-3′

Reverse

5′-TGGTGCGAATTCTGTGGATCGAACACAGGACCTCCAGATCTTCAGTC TGG-3′

$tRNA^{Trp}$ transcript

Forward

5′-**GGGTAATACGACTCACTATA**GAAGCGGTGGCTCAATGGTAGAGCTTT CGACTCCAAATC-3′

Reverse

5′-TGGTGAAACGGACAGGAATTGAACCTGCAACCCTTCGATTTGGAGTC GAAAGCTCTAC-3′

G34A

Forward

5-′**GGGTAATACGACTCACTATA**GCGGATTTAGCTCAGTTGGGAGAGCGC CAGACTAAAGATCTGGAGGTC-3′

Reverse

5′-TGGTGCGAATTCTGTGGATCGAACACAGGACCTCCAGATCTTTAGTC TGG-3′

G34C

Forward

5′-**GGGTAATACGACTCACTATA**GCGGATTTAGCTCAGTTGGGAGAGCGC C AGACTCAAGATCTGGAGGTC-3′

Reverse

5′-TGGTGCGAATTCTGTGGATCGAACACAGGACCTCCAGATCTTGAGTC TGG-3′

G34U

Forward

5′-**GGGTAATACGACTCACTATA**GCGGATTTAGCTCAGTTGGGAGAGCGC CAGACTTAAGATCTGGAGGTC-3′

Reverse

5′-TGGTGCGAATTCTGTGGATCGAACACAGGACCTCCAGATCTTAAGTC TGG-3′

Δ D-arm

Forward

5′-**TAATACGACTCACTATA**GCGGATTTAGCGCCAGACTGAAGATCTGGA GGTCCTGTGT-3′

Reverse

5′-TGGTGCGAATTCTGTGGATCGAACACAGGACCTCCAGATCTT-3′

Δ T-arm

Forward

5′-**TAATACGACTCACTATA**GCGGATTTAGCTCAGTTGGGAGAGCGCCAG ACTGA-3′

Reverse

5′-TGGTGCGAATTCGGACCTCCAGATCTTCAGTCTGGCGCTCTCCC-3′

Δ anticodon-arm

Forward

5′-**TAATACGACTCACTATA**GCGGATTTAGCTCAGTTGGGAGAGCGCGAG GTCCTGTGT-3′

Reverse

5′-TGGTGCGAATTCTGTGGATCGAACACAGGACCTCGCGCTCTCC-3′

Δ aminoacyl-stem

Forward

5′-**TAATACGACTCACTATA**GGTAGCTCAGTTGGGAGAGCGCCAGACTGA AGATCTGGAG-3′

Reverse

5′-CTGTGGATCGAACACAGGACCTCCAGATCTTCAGTCTGGCGC-3′

The bold show a promoter that is recognized by T7 RNA polymerase. Mutational site colored red.

Supplementary Table S4. SAS data acquisition, sample details, data analysis, modelling fitting and software used.

A. Sample details		
	Trm7-Trm734	Trm7-Trm734-tRNA^{Phe}
Organism	*S. cerevisiae*	
Source (Catalogue No. or reference)	*E.coli* expressed	
Uniprot ID + (residues, tRNA)	P38238 (1-310), Q08924 (1-1013)	
Extinction coefficient (A_{280nm}, Abs $_{0.1\%}$ (w/v))	1.143	1.394
Partial specific volume $\bar{\upsilon}$ ($cm^3\ g^{-1}$)	0.737	0.714
mean scattering contrast $\Delta\bar{\rho}$ (cm^{-2})	2.683×10^{10}	3.019×10^{10}
M from chemical composition (Da)	147000	183000
concentration, (mg ml^{-1})	0.465, 0.62, 1.24, 1.86, 2.48, 3.10	1.22, 244, 3.66, 4.88, 6.10
Concentration values measured and method	Blood ford	
Solvent composition	50 mM HEPES-KOH, 200 mM, KCl, 5 % v/v glycerol, 10 mM β-mercaptoethanol, pH 8.0	
B. SAS data collection parameters		
Source, instrument	Photon Factory BL-10C	SPring 8 BL45XU
Wavelength (Å)	1.0	1.0
Camera Length (mm)	2050.38	1987.86
Beam geometry (μm)	V350 × H550	V150 × H350
	Bent cylindrical mirror + 2 slits + 1 pinhole	K-B mirror + 2slits + 1 pinhole
q-measurement range ($Å^{-1}$)	0.0095-0.4094	0.0071-0.4141
Absolute scaling method	Comparison with scattering from pure H_2O	
Basis for normalization to constant counts	Normalized to incident intensity by μ ion chamber	
Method for monitoring radiation damage	data frame-by-frame comparison	
Exposure time, number of exposures	10 sec, 40 images	1 sec, 20 images
Sample configuration including path length	1.25 mm	3 mm
Sample temperature (K)	293	293

C. Software employed for SAS data reduction, analysis and interpretation	
SAS data processing	*SAngler*
Extrapolation	*PRIMUSqt*
Calculation of ε from sequence	*ExPASy* (1)
Calculation of M.W. from scattering	*SAXSMoW*(v2.1)[8]
Calculation of $\Delta\overline{\rho}$ values	*MULCh* (2)
Calculation of $\overline{\upsilon}$ values	
Basic analyses: (Guinier, P(r), Porod Volume)	*PRIMUSqt*
Rigid body modelling with flexible linkers	*CORAL*

D. Structural parameters		
	Trm7-Trm734	Trm7-Trm734-tRNA^{Phe}
Guinier Analysis		
$I(0)$ (cm^{-1})	0.19 +/- 0.0003	0.27 +/- 0.0003
R_g (Å)	37.9 +/- 0.8	40.9 +/- 0.2
Q-range (Å^{-1})	0.0095-0.034	0.0071-0.032
$P(r)$ analysis		
$I(0)$ (cm^{-1})	0.19 +/- 0.0001	0.27 +/- 0.0005
R_g (Å)	37.67 +/- 0.03	40.98 +/- 0.11
D_{max} (Å)	130	155
Q-range (Å^{-1})	0.01265 - 0.32383	0.01957 - 0.32424
M from $I(0)$ (ratio to expected value)	158819 (1.08)	177332 (0.97)
M compared with Ovalbmin	151430 (1.03)	208060 (1.14)
V_p, M from V_p (ratio to expected value)	218000, 136250 (0.93)	254000, 158750 (0.87)

E. Shape modelling results	
	Trm7-Trm734
DAMMIF(default parameters, 20 calculations)	
Q-range for fitting	0.01265 - 0.32383
Symmetry/anisotropy assumptions	*P*1, none
NSD (standard deviation), No of clusters	1.05 (0.06), 1
χ^2 range	1.909 - 1.957
Model *M* estimate ($\times 0.5\ V_{model}$) (Da)	137000
Model resolution (Å)	48 +/- 4
DAMMIN (default parameters)	
Q-range for fitting	0.01265 - 0.32383
Symmetry/anisotropy assumptions	*P*1
χ^2 value, *CORMAP P* value	1.92, 0.03
Constant adjustment to intensities	2.38×10^{-4}
F. Rigid body modelling	
	Trm7-Trm734
CORAL (default parameters)	
Q-range for all modelling	0.01265 - 0.32383
Symmetry assumptions	*P*1
χ^2 value, *P* value	2.18, 0.00
Constant adjustment to intensities	3.04×10^{-4}
Domain coordinates	Trm7 / Trm734
Domain contacts	12 Å for Trm734/Trm7
	(residue: 111-112/138-140)
regions of presumed flexibility	Residue 1-8, 260-310 of Trm7
F. Data and model deposition IDs	
Trm7-Trm734	SASDDR3

Supplementary Table S5.

Interface residues of Trm7 interacted with BPA and BPC in Trm734.

Trm7	Accessible surface area (Å^2)	Buried surface area (Å^2)	Trm734 domain
R14	147.16	0.58	BPC
L84	115.82	28.18	BPA
T101	87.05	0.34	BPA
H102	121.87	1.59	BPA
P127	60.15	11.16	BPA
D128	136.84	10.7	BPA
V129	105.08	16.6	BPA
T130	93.94	84.58	BPA
G131	48.63	23.19	BPA
L132	110.87	92.35	BPA
H133	110.46	81.21	BPA
D134	87.76	68.2	BPA
L135	77.14	53.17	BPA
E137	11.4	0.12	BPA
Y138	132.27	96.46	BPA
V139	38.67	28.79	BPA
Q142	91.33	68.54	BPA
L143	54.64	2.0	BPA
R167	103.06	98.26	BPC
G168	25.77	22.11	BPC
R169	171.21	146.18	BPC
I171	19.9	16.91	BPC
D172	29.52	16.46	BPC
M173	34.47	14.96	BPC
Y175	16.11	6.92	BPC
C187	3.49	0.5	BPC
K189	50	22.93	BPC
R191	130.6	25.32	BPC

G195	78.11	11.21	BPC
T196	128.45	33.49	BPC
L198	84.85	53.74	BPC
N233	202.11	152.65	BPA
K234	176.45	10.23	BPA
C236	75.67	34.25	BPA
S238	48.26	20.12	BPA
D239	90.5	49.19	BPA
S242	36.77	18.58	BPA
E246	66.27	10.75	BPA
E247	115.3	31.46	BPA
R249	114.13	44.85	BPC
I251	158.65	91.97	BPC
A252	15.59	2.45	BPC
F254	101.27	83.98	BPC
M255	64.63	6.86	BPC
A256	54.08	34.58	BPC
Total	3826.3	1728.67	

Supplementary Table S6.

Interface residues of Trm734 interacted withTrm7.

Trm734	Trm734 domain	Accessible surface area (Å^2)	Buried surface area (Å^2)
P9	Linker	6.36	2.68
L11	BPA	23.34	14.47
Y47	BPA	94.71	45.51
N48	BPA	27.96	22.99
K49	BPA	35.38	16.6
H51	BPA	65.72	33.78
A66	BPA	13.31	8.17
R67	BPA	113.34	72.72
I89	BPA	85.45	7.6
S91	BPA	88.63	33.36
D92	BPA	44.69	23.2
W93	BPA	111.05	92.35
C111	BPA	15.63	12.45
Y112	BPA	67.3	53.3
N113	BPA	8.07	1.49
K114	BPA	73.28	28.19
S129	BPA	33.54	2.64
L130	BPA	44.51	15.67
G131	BPA	74.23	0.48
G132	BPA	70.91	20.32
E133	BPA	159.29	9.87
R134	BPA	155.78	86.33
S135	BPA	24.28	0.73
I136	BPA	91.27	20.9
L137	BPA	6.38	0.37
Y138	BPA	117.15	73.78
M158	BPA	169.22	26.6
F183	BPA	41.94	24.05

R223	BPA	82.09	53.71
W225	BPA	32.28	14.56
E241	BPA	13.23	0.12
K272	BPA	64.01	8.87
S273	BPA	4.72	2.82
W275	BPA	70.29	53.26
N291	BPA	23.13	10.28
E656	BPC	26.76	5.77
R658	BPC	94.55	24.69
E685	BPC	57.3	6.62
D763	BPC	163.87	0.73
F817	BPC	47.21	3.75
T835	BPC	42.08	11.44
D836	BPC	50.55	3.5
Q882	BPC	162.52	73.42
S883	BPC	41.08	27.08
K886	BPC	57.87	8.03
D906	BPC	65.33	53.64
D907	BPC	27.48	20.32
N908	BPC	40.91	34.36
A933	BPC	85.08	29.75
A935	BPC	8.91	7.74
S936	BPC	90.74	84.17
S937	BPC	36.06	35.45
T938	BPC	25.54	10.54
V956	BPC	51.97	44.18
D957	BPC	26.71	25.41
Q958	BPC	56.8	40.66
R961	BPC	23.55	1.32
R977	BPC	126.73	51.53
T978	BPC	4.45	0.12
A981	BPC	30.63	27.28

D982	BPC	59.85	36.39
V1006	BPC	25.73	19.75
Total		3682.73	1581.86

Legends to Supplementary Figures

Supplementary Figure S1. SDS-PAGE (12.5%) of the purified recombinant Trm7-Trm732. The gel was stained with Coomassie Brilliant Blue.

Supplementary Figure S2. Two-dimensional thin-layer chromatographic analysis of methylated nucleosides. The ^{14}C-methylated *Saccharomyces cerevisiae* tRNA^{Phe} transcript modified with Cm32 and m^{1}G37 by Trm7-Trm734 was digested with Nuclease P1 at 37ºC for 12 h. The nucleotides were separated by two-dimensional thin-layer chromatography using the following two solvent systems: (A) first dimension, isobutyric acid/concentrated ammonia/water, 66:1:33, v/v; second dimension, isopropyl alcohol/HCl/water, 70:15:15, v/v; (B) first dimension, isobutyric acid/concentrated ammonia/water, 66:1:33, v/v/v; second dimension, 0.1 M Sodium phosphate (pH 6.8), ammonium sulfate, n-propanol, 100:60:2, v/w/v, and then the ^{14}C-methylated nucleotides were detected by autoradiography. The standard markers (pA, pG, pC and pU) were detected by UV254nm irradiation. ^{14}C-pGm spots are enclosed by red dotted circles.

Supplementary Figure S3. (A) *Left*, ribbon models of two Trm7-Trm734-SAM complexes in an asymmetric unit of the crystal belonging to the monoclinic *C2* space group. The Trm7, Trm734 BPA, BPB and BPC are colored red, green, blue and yellow, respectively. *Right*, line diagrams of the structure in left pannels. One Trm7-Trm734 is colored magenta, another is colored cyan. Ball models show the HEPES (cyan) and sulfate (orange). (B) Ribbon diagram of the heterodimer of Trm7-Trm734-SAM complex including one HEPES and five sulfates.

Supplementary Figure S4. Close-up view of the large space (dotted red-circle) consisting of interacting Trm7-Trm734 molecules in the crystal with non-crystallographic symmetry.

Supplementary Figure S5. Profiles contributed to SAXS experiments. Black and blue lines are attributed to Trm7-Trm734 and Trm7-Trm734-tRNA^{Phe} respectively. (A) log $I(Q)$ versus Q plots. Red line superposed to the black line is corresponding to the theoretical scattering curve calculated from rigid body model of Trm7-Trm734 obtained by *CORAL*. These χ^2 values are 2.18 for Trm7-Trm734. (B) Guinier plots. $Q \times R_g$ regions shown by continuous lines are

equivalent to $0.36 < Q \times R_g < 1.30$ for Trm7-Trm734 and $0.29 < Q \times R_g < 1.27$ for Trm7-Trm734-tRNA^{Phe} respectively. (C) Dimensionless Kratky plots. (D) Normalized pair distribution function. These maximum size parameters (D_{max}) are 130 Å for Trm7-Trm734 and 155 Å for Trm7-Trm734-tRNA^{Phe} respectively.

Supplementary Figure S6. Topology diagrams of Trm7 (A) and Trm734 (B). The α helices, 3_{10} helix, and β strands are labeled as α, 3_{10}, and β, respectively. The N- and C-terminal ends are indicated as N and C, respectively. The four antiparallel β strands of one WD40 blade are labeled as a, b, c, and d, respectively, in the three WD40 domains (BPA, green; BPB, blue; and BPC, yellow) of Trm734. The WD40 blades in the WD40 domain are numbered from 1 to 7.

Supplementary Figure S7. Structural information-based amino acid sequence alignments of *S. cerevisiae* Trm7, *Kluyveromyces marxianus* Trm7, *S. pombe* Trm7, *Arabitopsis thaliana* Trm7 and *H. sapiens* FTSJ1 and *E. coli* RlmE. Identical and similar residues are boxed. Secondary structure of the *S. cerevisiae* Trm7 and *E. coli* RlmE are indicated above and below the alignments. The position of A26P mutation in *H. sapiens* FTSJ1, which causes NSXLID, is

shown by black-arrow. This figure was created using ClustalW (15) and ESPript (16). The conserved residues responsible for interaction with SAM are colored green. The catalytic residues for methylation are colored blue labeled with blue-circles.

Supplementary Figure S8. Structural information-based amino acid sequence alignments of *S. cerevisiae* Trm734, *S. pombe* Trm734 and *H. sapiens* WD8. Identical and similar residues are boxed. Each secondary structures of the BPA (green), BPB (blue) and BPC (yellow) domains of *S. cerevisiae* Trm734 are indicated above the alignments. The minimal unit of the WD40 domain constitutes a four-stranded anti-parallel β-sheet (a, b, c, and d). This figure was created using ClustalW (15) and ESPript (16).

Supplementary Figure S9. (A) Line diagram of the superimposed Cα atoms of BPA in Trm734 (green) onto those of BPC in Trm734 (yellow) (r.m.s.d = 2.29 Å for 249 aligned residues). (B) Line diagram of superimposed Cα atoms of BPA in Trm734 (green) onto those of BPB in Trm734 (blue) (r.m.s.d = 3.39 Å for 211 aligned residues). (C) Line diagram of superimposed Cα atoms of BPB in Trm734 (green) onto those of BPC in Trm734 (yellow)

(r.m.s.d = 3.14 Å for 262 aligned residues).

Supplementary Figure S10. (A) Schematic diagram of detailed interactions between the residues of Trm7 and SAM. (B) Surface model of the SAM bound form of Trm7-Trm734. The degrees of conservation are represented by a gradient color between conserved (purple) and variable (cyan). White indicates areas in which conservation and variability average out. (C) Stick diagram of the four catalytic resides and SAM in *S. cerevisiae* Trm7 (green) superimposed onto those in *E. coli* RlmE (cyan).

Supplementary Figure S11. (A) Close-up view of the interacting residues (stick models) between Trm7 (red) and BPA of Trm734 (green). The dotted lines show hydrogen bonds and salt bridges between Trm7 and BPA of Trm734. Detailed distances for the interaction are tabulated in Table 2A. (B) Close-up view of the interacting residues (stick models) between Trm7 (red) and BPC of Trm734 (yellow). The dotted lines show hydrogen bonds and salt bridges between Trm7 and BPC of Trm734. Detailed distances for the interaction are tabulated in Table 2B.

Supplementary Figure S12. (A) Ribbon diagram of the overall structure of human DDB1-DDB2-DNA complex (PDBID = 3El1). The three WD40 domains of DDB1-BPA, DDB1-BPB and DDB1-BPC are colored red, purple and orange, respectively. The CTD of the

DDB1 and WD40 domain of DDB2 are colored gray and green, respectively. The double stranded DNA bound to DDB2 is shown by a stick model. (B) Surface model of DDB1 structure and its cartoon model. The shallow cleft consisting of DDB1-BPA and DDB1-BPC (dotted black-circle) is responsible for interacting with the DDB2.

Supplementary Figure S13. (A) Cloverleaf structure of *Saccharomyces cerevisiae* $tRNA^{Phe}$ and four mutant $tRNA^{Phe}$ transcripts (ΔD-arm, ΔT-arm, Δanticodon-arm and Δaminoacyl-stem) (B) The autoradiogram of the same gel, shown in panel A.

Supplementary Figure S1

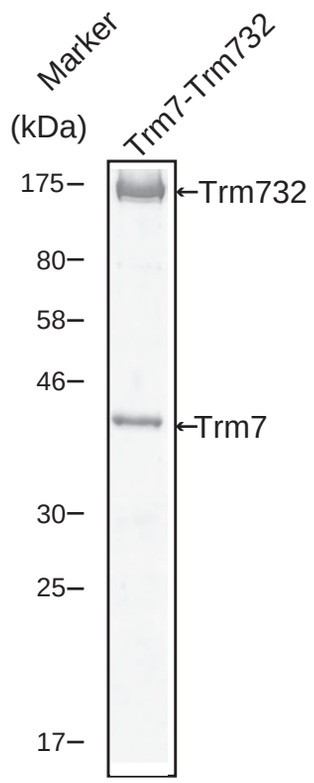

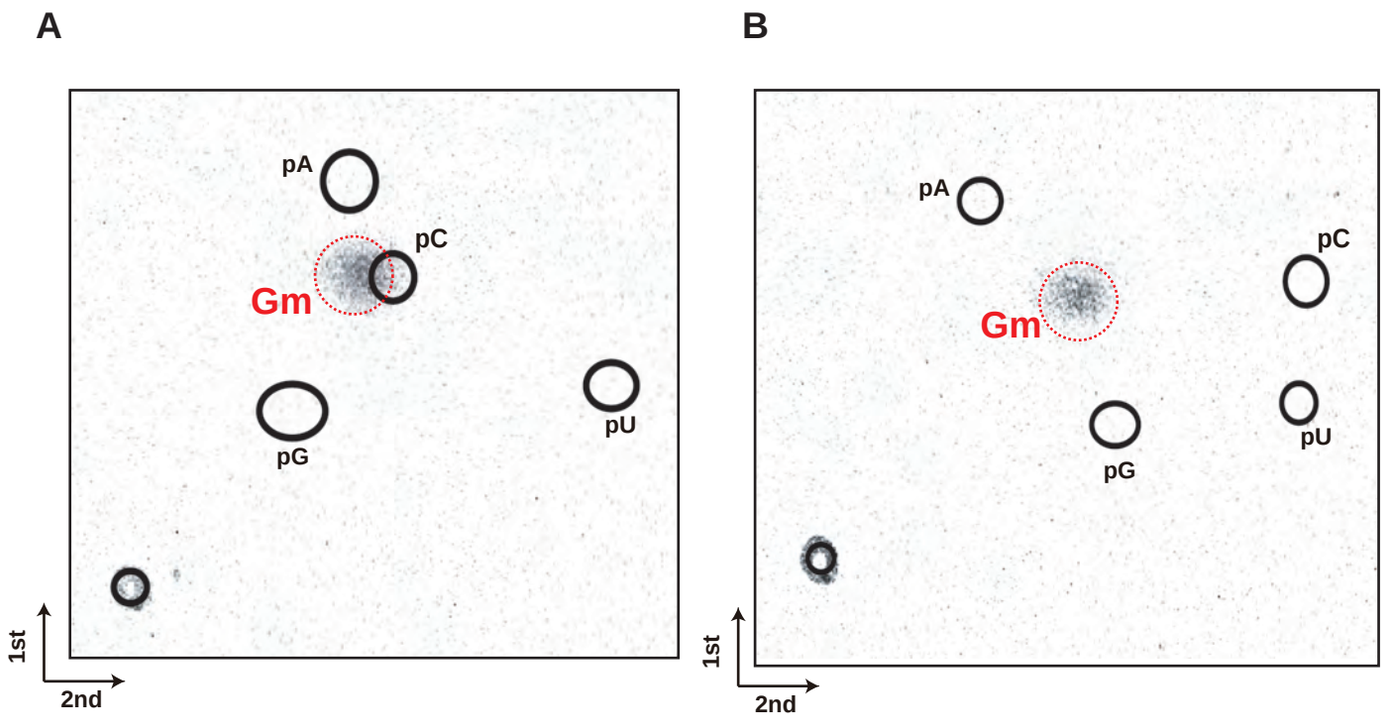

Supplementary Figure S2

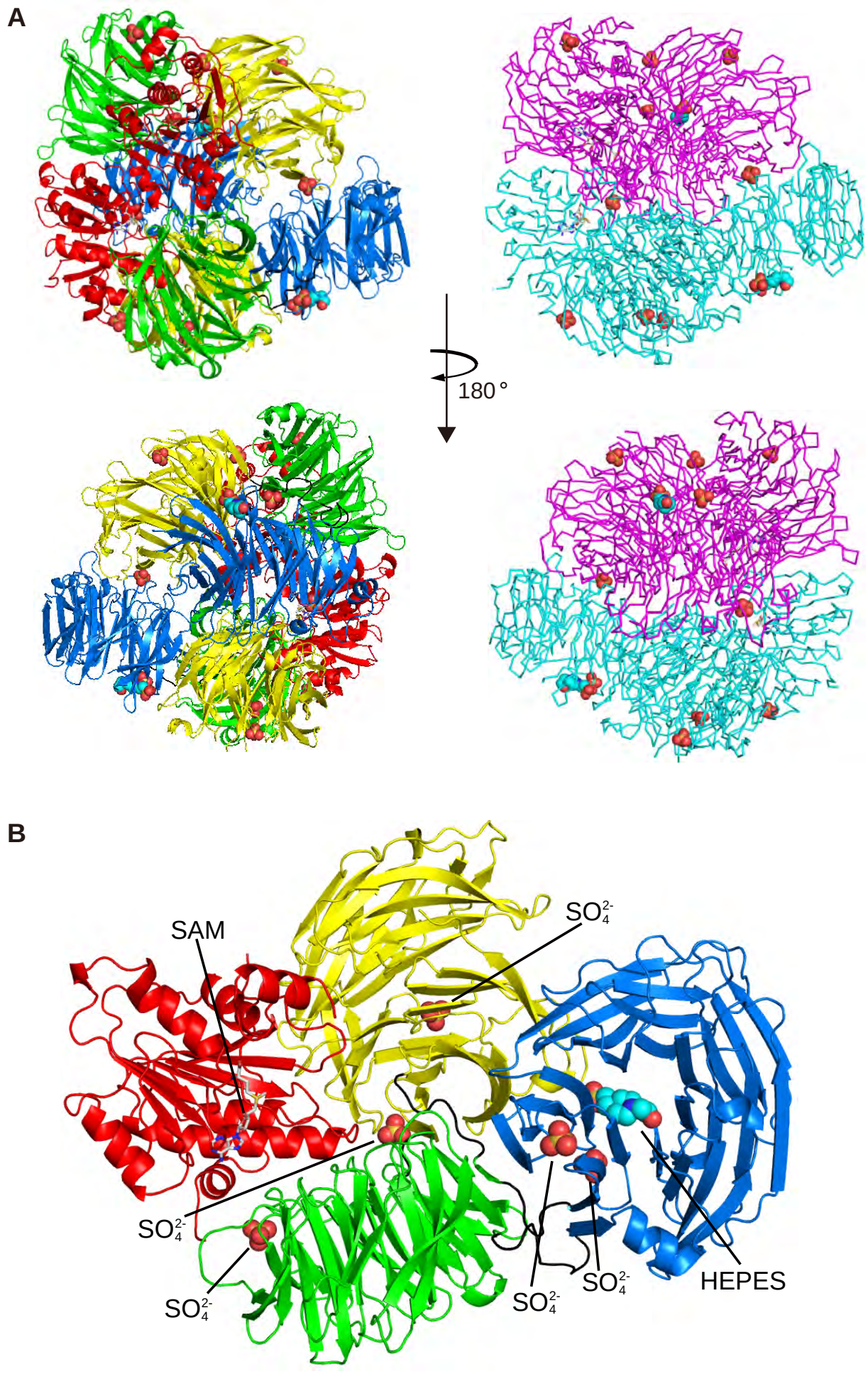

Supplementary Figure S3

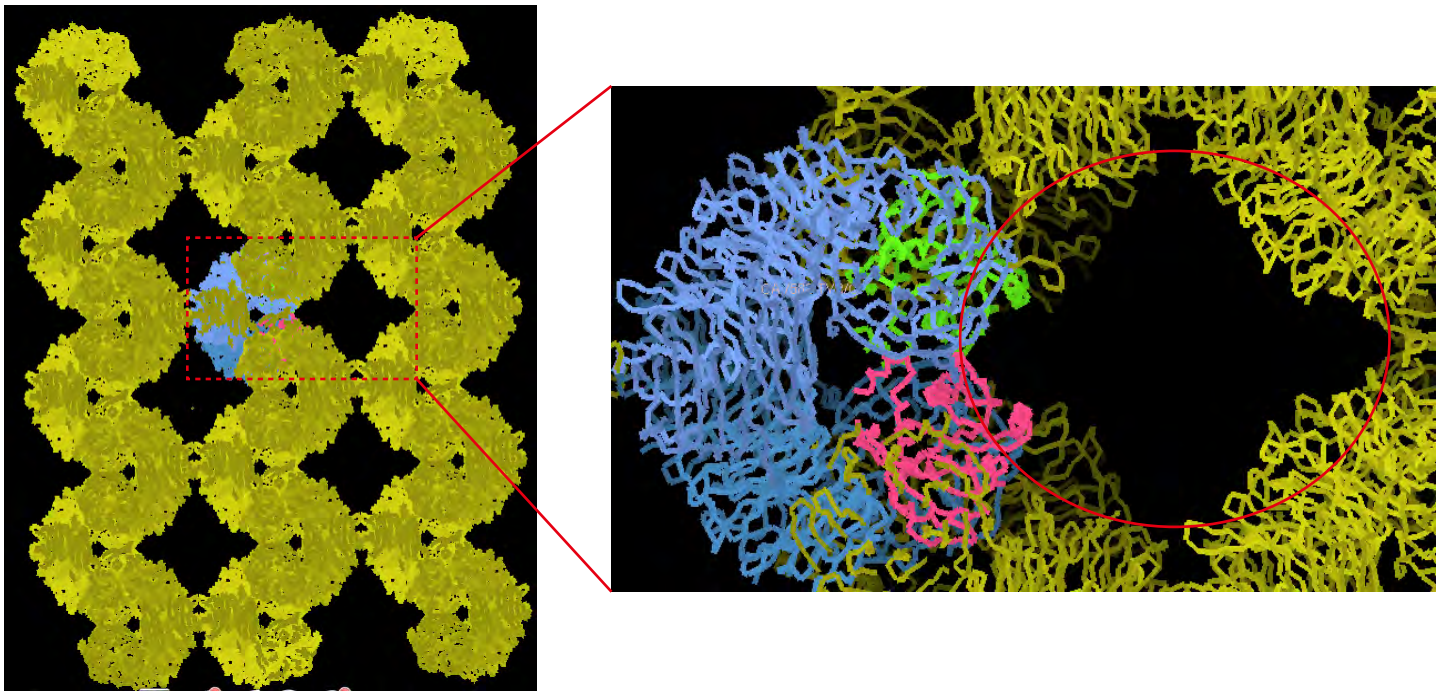

Supplementary Figure S4

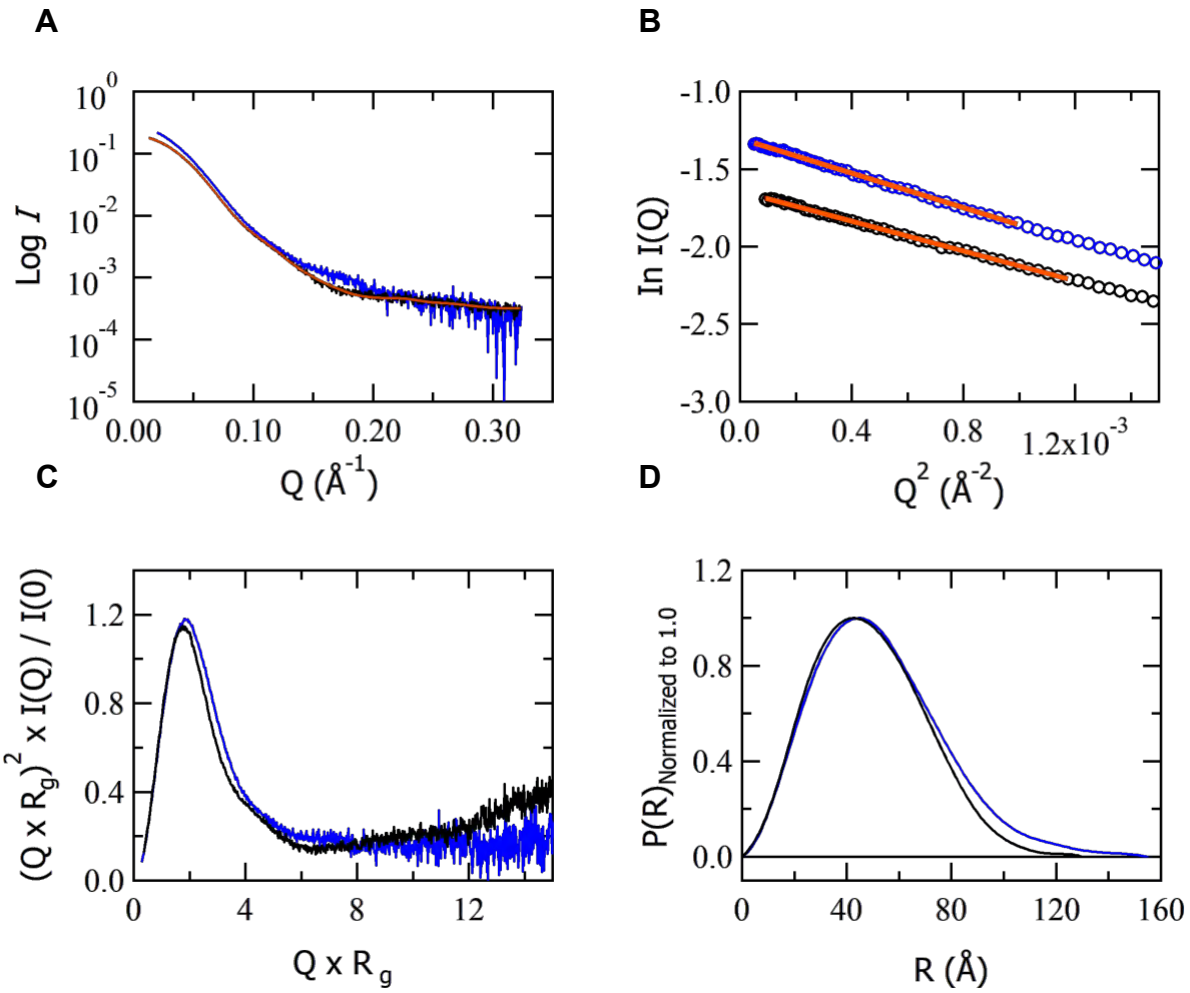

Supplementary Figure S5

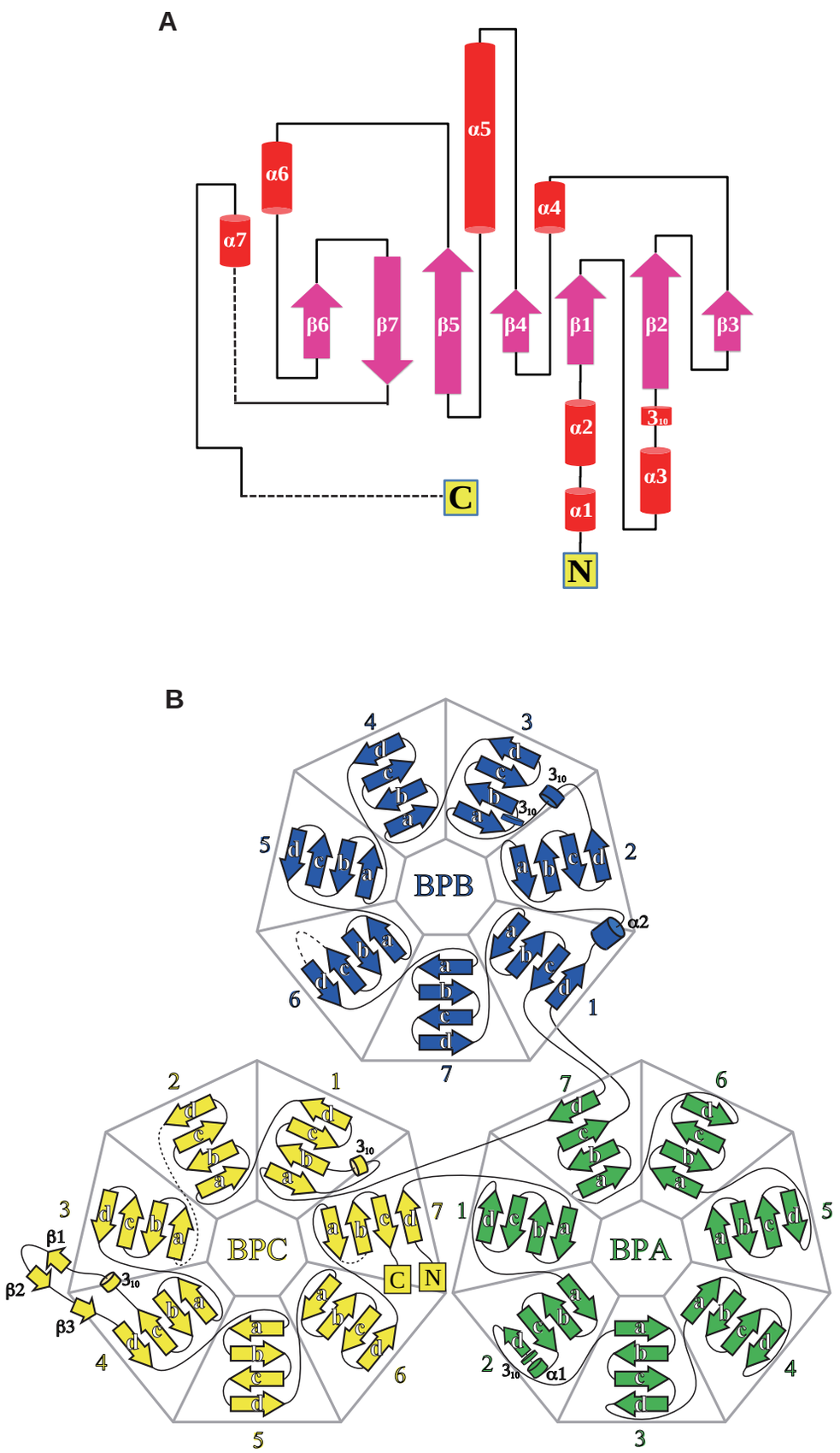

Supplementary Figure S6

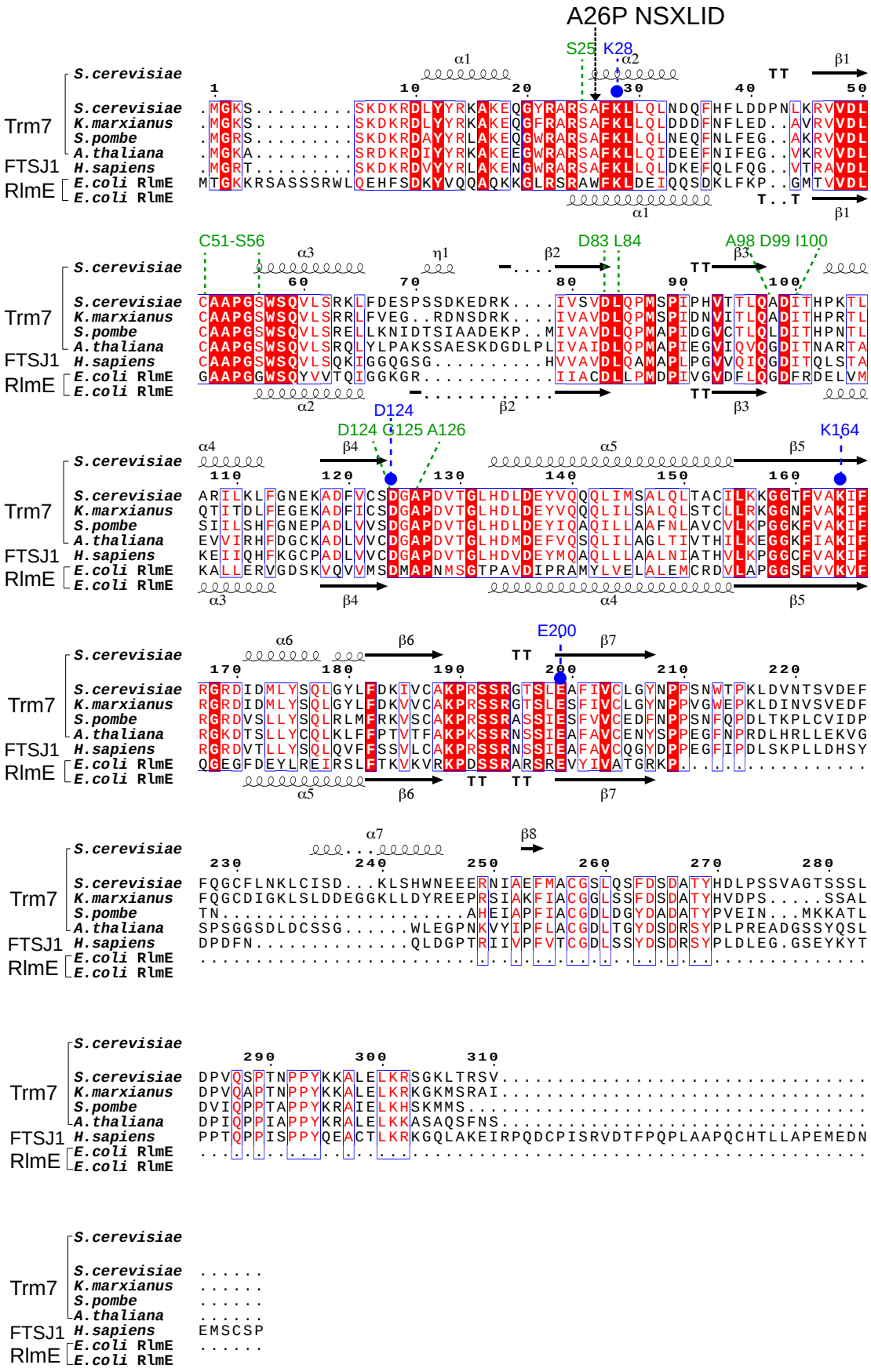

Supplementary Figure S7

Supplementary Figure S8

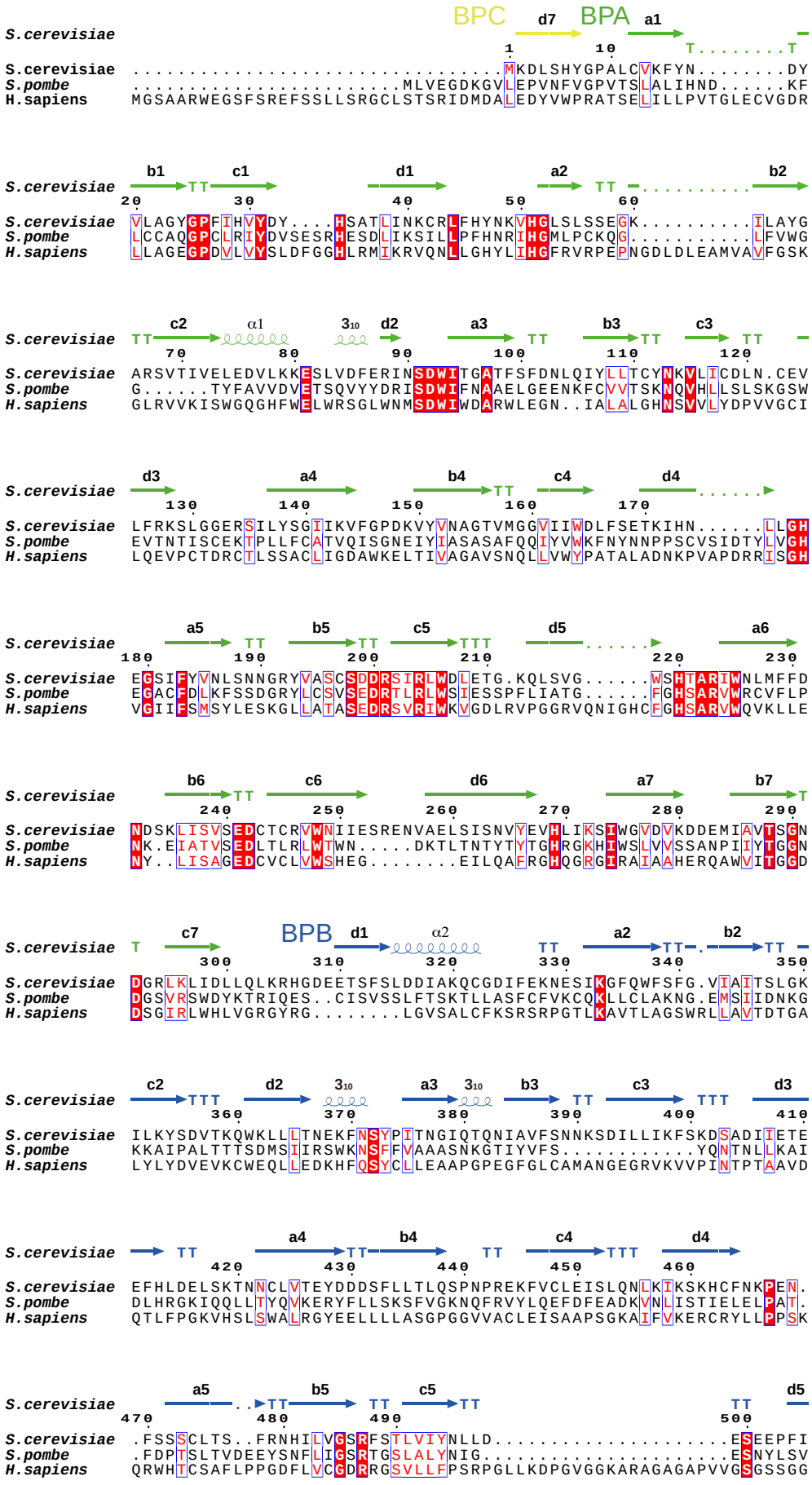

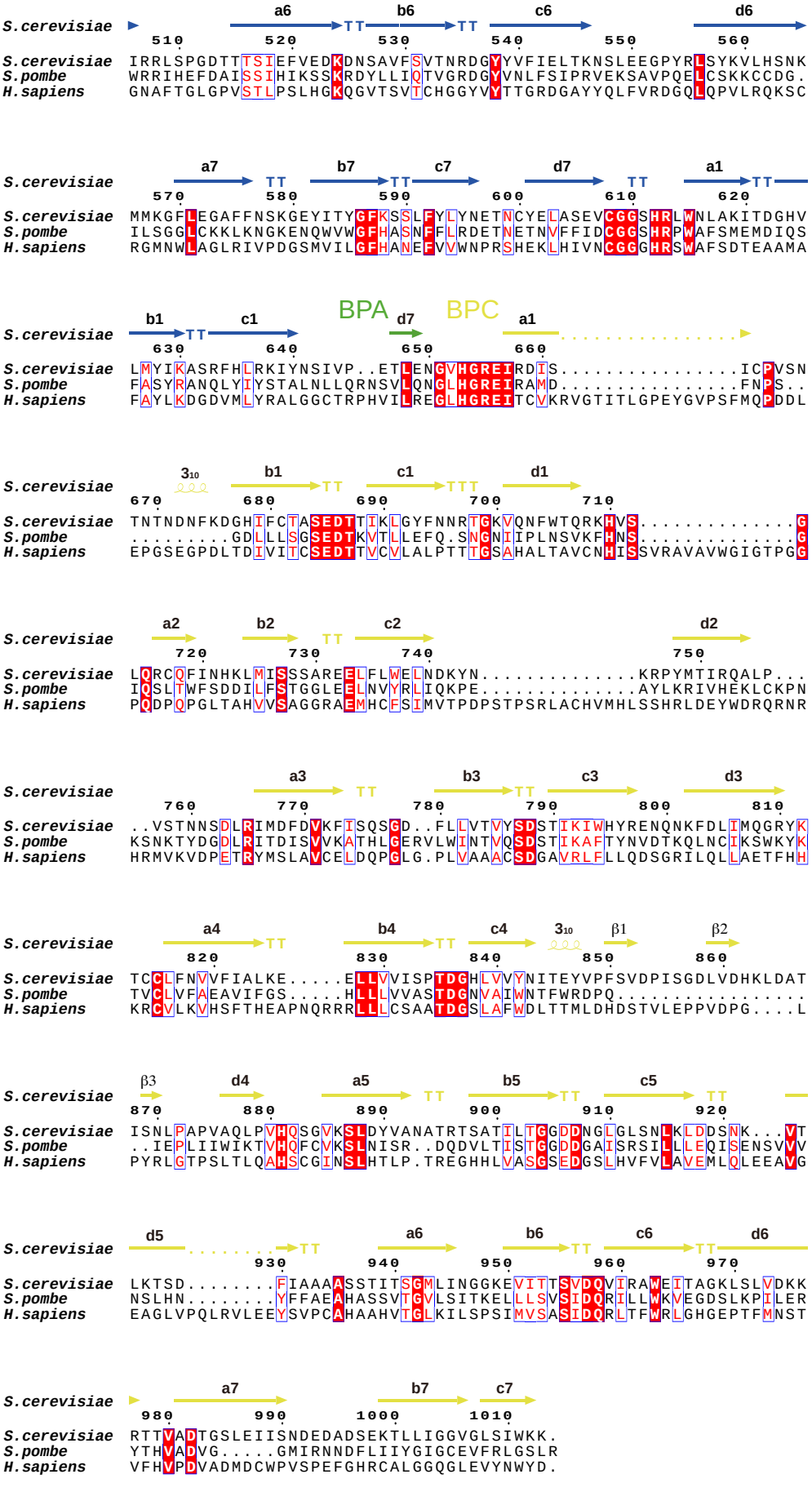
S.cerevisiae
S.pombe
H.sapiens
BPA
BPC

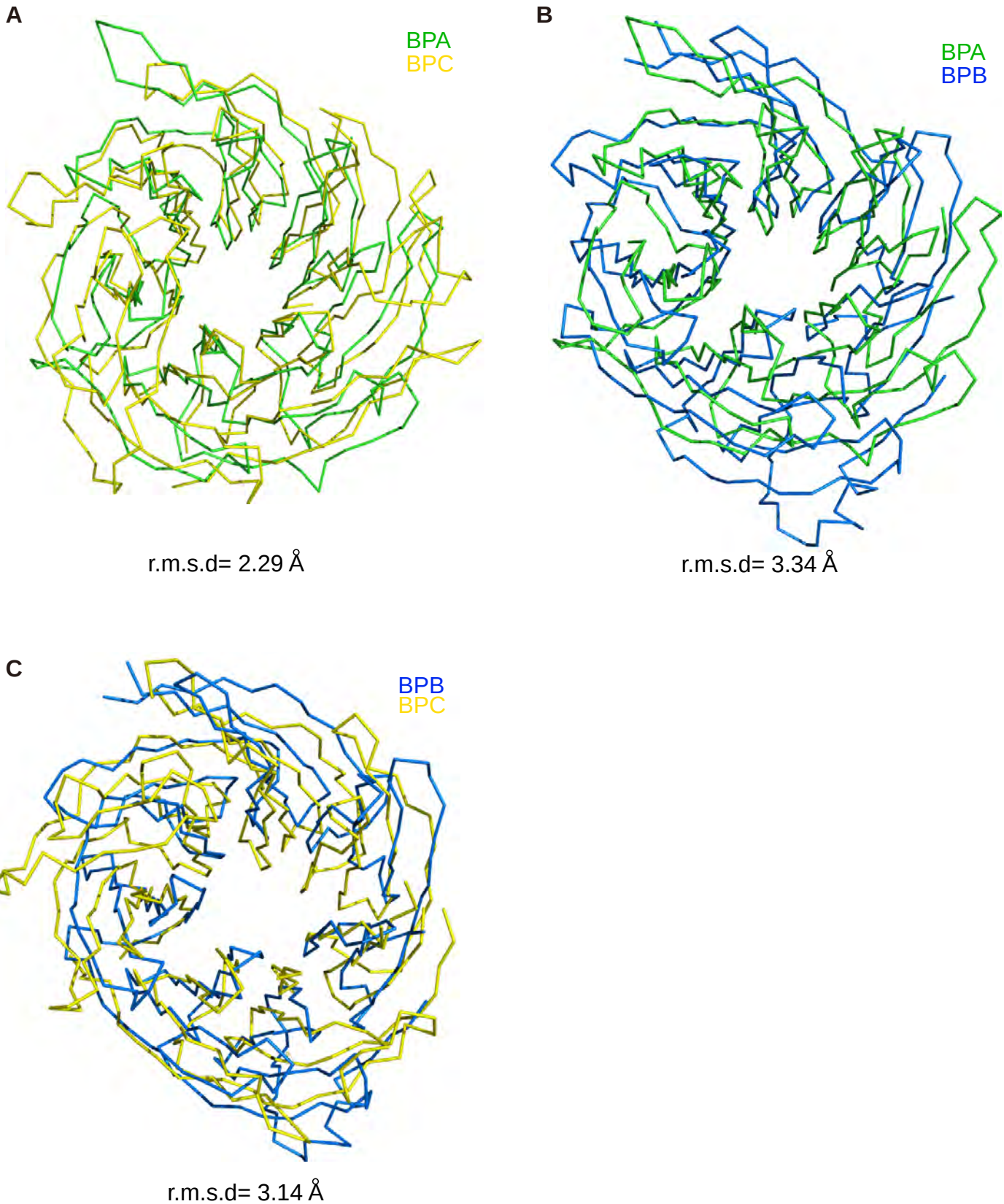

Supplementary Figure S9

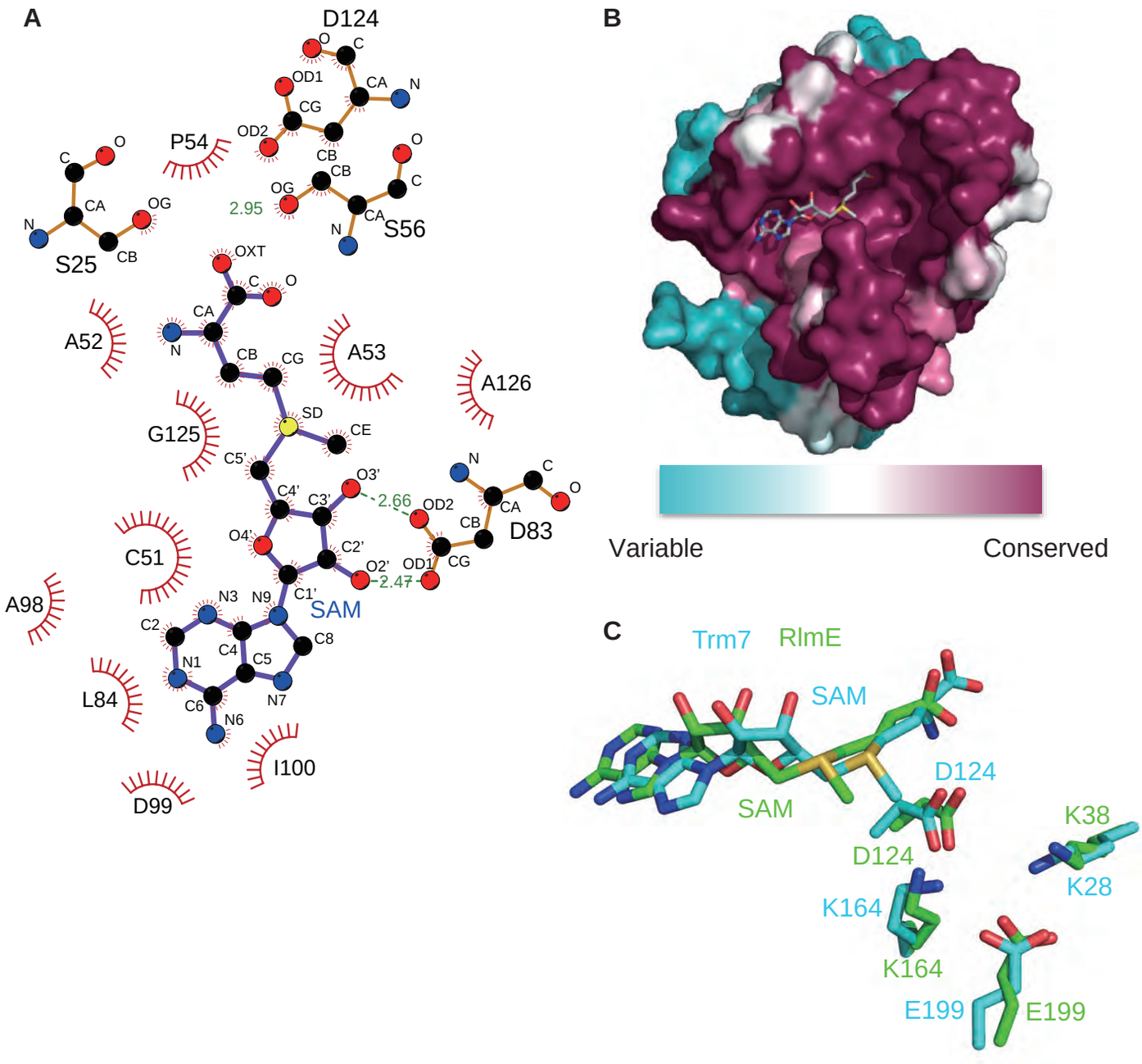

Supplementary Figure S10

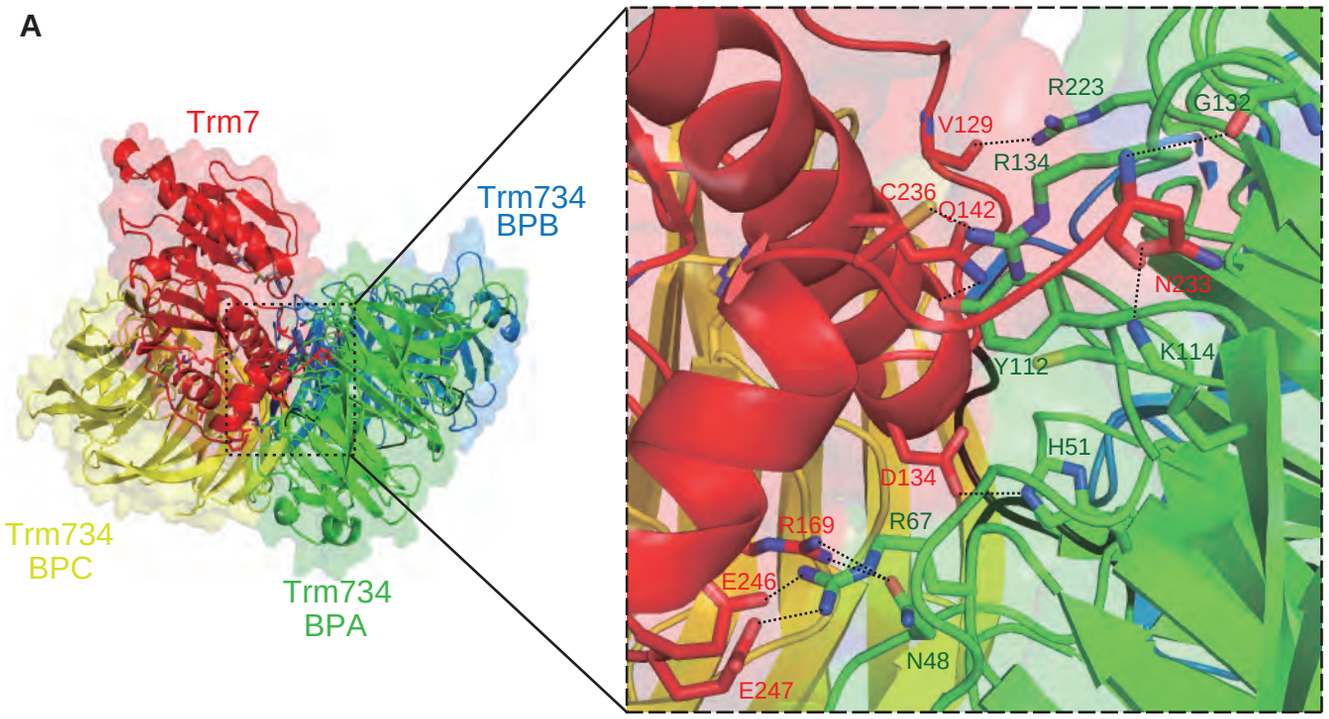

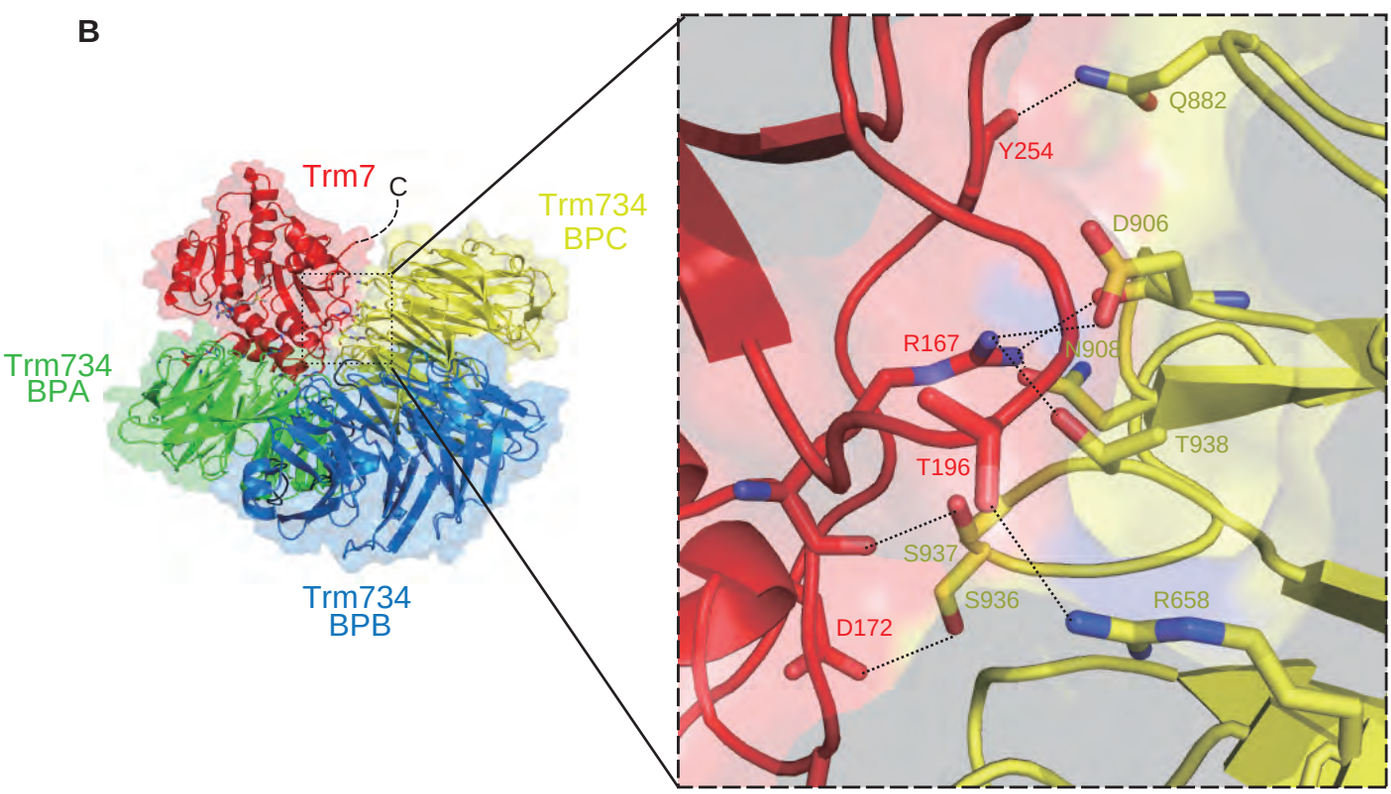

Supplementary Figure S11

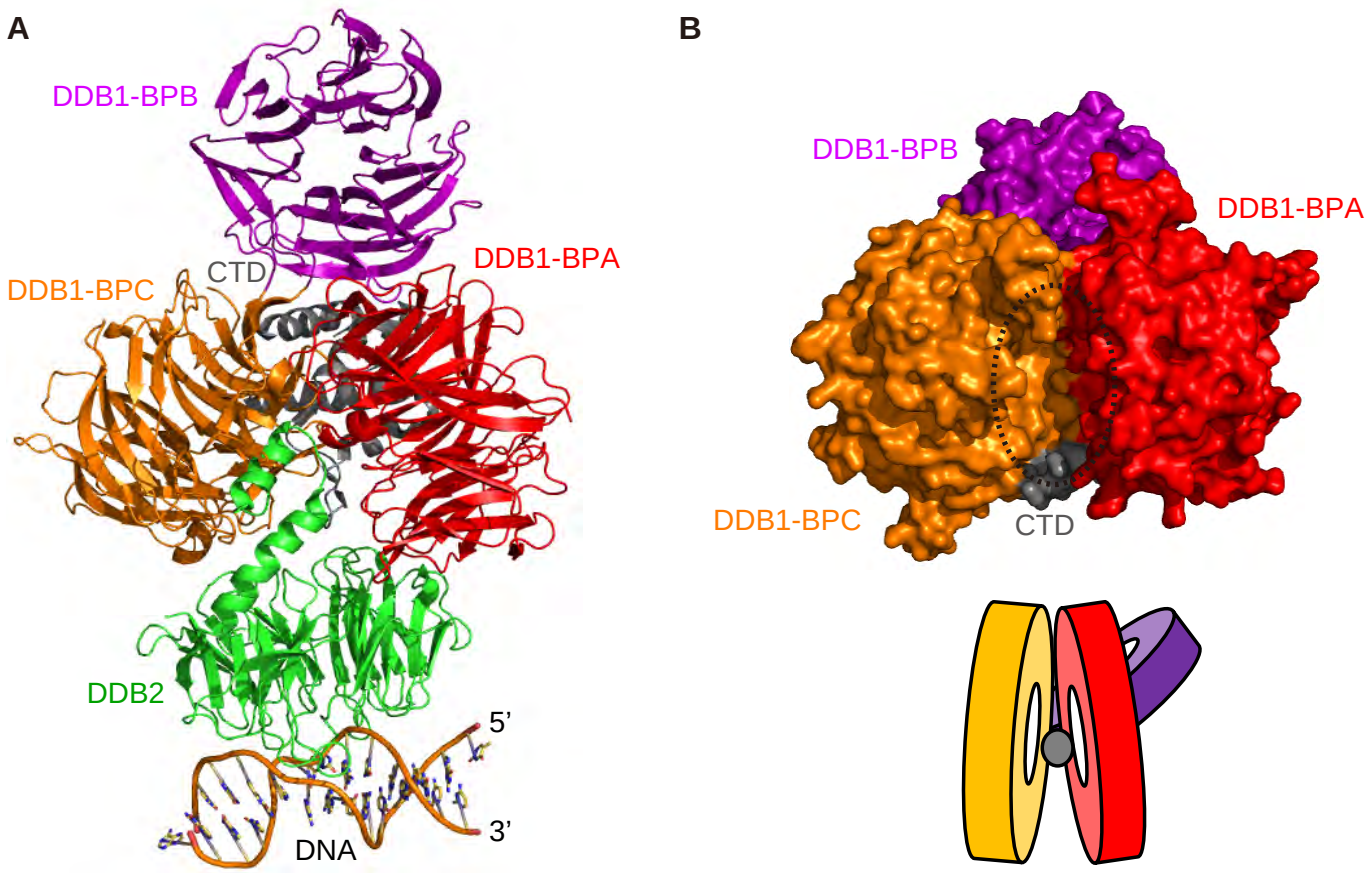

Supplementary Figure S12

Supplementary Figure S13

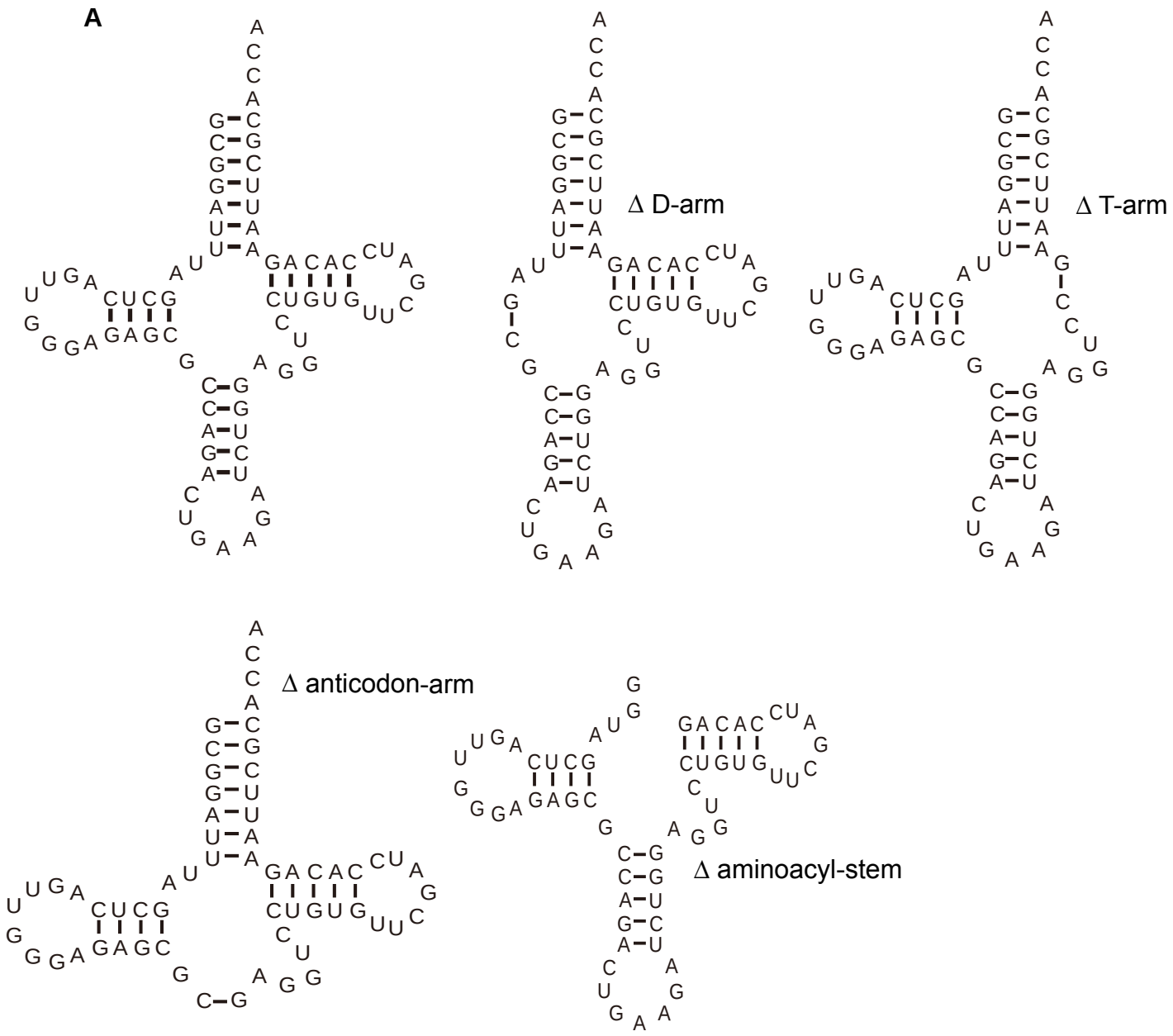

10% PAGE 7M Urea **Autoradiogram**